

# Physical Layer Frame in Signalling-Data Separation Architecture: Overhead and Performance Evaluation

Abdelrahim Mohamed\*, Oluwakayode Onireti\*, Yanan Qi\*, Ali Imran†, Muhammed Imran\*, Rahim Tafazolli\*

\*Centre for Communication Systems Research CCSR  
University of Surrey  
Guildford, UK

†Telecommunication Engineering  
University of Oklahoma  
Tulsa, USA

E-mail: {abdelrahim.mohamed; o.s.onireti; yinan.qi; m.imran; r.tafazolli} @ surrey.ac.uk

E-mail: dr.ali.imran @ ieee.org

**Abstract**—Conventional cellular systems are dimensioned according to a worst case scenario, and they are designed to ensure ubiquitous coverage with an always-present wireless channel irrespective of the spatial and temporal demand of service. A more energy conscious approach will require an adaptive system with a minimum amount of overhead that is available at all locations and all times but becomes functional only when needed. This approach suggests a new clean slate system architecture with a logical separation between the ability to establish availability of the network and the ability to provide functionality or service. Focusing on the physical layer frame of such an architecture, this paper discusses and formulates the overhead reduction that can be achieved in next generation cellular systems as compared with the Long Term Evolution (LTE). Considering channel estimation as a performance metric whilst conforming to time and frequency constraints of pilots spacing, we show that the overhead gain does not come at the expense of performance degradation.

**Index Terms**—Base stations; energy efficiency; equalizer; GSM; interpolation; OFDM; physical layer; radio access networks

## I. INTRODUCTION

Nowadays, the Information and Communication Technology (ICT) sector is responsible of 2% of the global emissions and this contribution is expected to double every five years [1]. In wireless systems, most of the energy is consumed by radio interface components such as the base station (BS) [2]. Hence energy considerations call for the design of efficient, adaptive and environmental friendly radio access networks. Conventional cellular systems consume high power even in low traffic situations because they continuously transmit control and reference signals to provide ubiquitous coverage or “always-on” system. In contrast to this approach, an “on demand” system scales the energy consumption with the traffic load but it creates coverage holes [3]. Thus a new cellular architecture based on both the always-on and the on demand systems can provide an energy efficient and “always available” system. The key concept behind this architecture is that only small amount of signalling information is required to provide full coverage while the control information related to data transmission is required only when there are active users [3]. As a result, the signalling plane can be separated from the data

plane without affecting the availability of the network, which will result in order of magnitude savings in energy.

Considering this architecture as a candidate for next generation (NG) cellular systems [4] and taking into account that dense deployment of small cells is the most promising solution to satisfy the exponentially increasing traffic demand [5], of great importance is the design of a new physical layer (PL) frame optimized for such deployments. In current systems, all cells (i.e., macro, micro, pico, etc.) use a unified frame structure optimized for macro coverage. In addition, a worst-case scenario, e.g., high mobility assumption, is adopted in dimensioning the PL frame. Although this approach ensures good performance for users under such severe conditions, it wastes the valuable power and bandwidth resources by over-provisioning the frame for other users under moderate or good channel conditions. Minimizing the energy consumption and meeting the ambitious 10 Gb/s peak data rate target of 5G cellular systems [6] motivate the design of a power and bandwidth efficient PL frame with a minimum amount of overhead. It is worth mentioning that the signalling-data separation architecture has been proposed in the EARTH project [2] and it is being investigated in several projects that aim to define the enabling technologies for fifth generation cellular systems. Reference [7] proposes a functionality separation scheme and proves that this architecture provides significant energy saving as compared with existing systems. The work conducted in [8] provides a splitting scheme for the GSM while [3] and [9] discuss the advantages and technical challenges of this architecture. Although [3], [7]–[9] show potential benefits of the separation architecture from energy perspective, they do not compare its performance gain/penalty with the existing state of the art systems. A new carrier type, known as Lean Carrier, has been proposed in [10] for the Long Term Evolution (LTE) to allow switching off the BS transmission circuitry during unoccupied subframes. From overhead perspective, [11] focuses on the time dimension and proposes a physical subframe optimized for local area (LA) environment. It takes into account latency and overhead requirements of NG cellular systems as well as the expected technological evolution in the next decade. Although [11] shows a significant overhead and latency reduction as compared with the LTE and WIMAX,

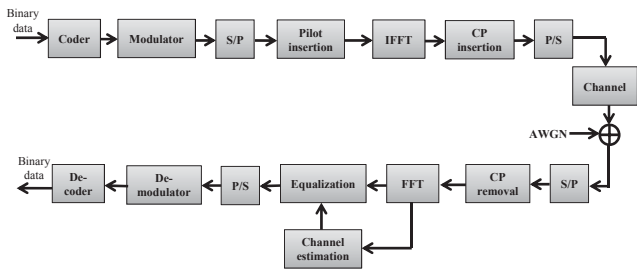


Fig. 1. Block diagram of a baseband OFDM system

the subframe has not been provisioned for the separation architecture and reference signals (RS) allocations as well as the performance gain/penalty have not been addressed.

In this paper, we show that the classical approach of using a unified frame structure optimized for macro coverage results into redundant overhead without significant performance gain in futuristic small cell deployment scenarios. We adopt the subframe structure proposed in [11] and allocate the control signals according to the separation scheme proposed in [7]. Leaving the adaptive allocation techniques to a separate study, we determine the appropriate pilot pattern for small and macro cells based on their design limits and compare the overhead as well as the performance in each case with the LTE. The remainder of this paper is organized as follows: Section II describes the LTE system model along with the channel estimation method and formulates the overhead of its PL subframe. Section III describes a signalling-data separation scheme and formulates the overhead of a proposed NG subframe. Section IV provides allocation examples while Section V shows and discusses simulation results. Finally, Section VI concludes the paper by providing an overall conclusion.

## II. LTE SYSTEM MODEL AND FRAME NUMEROLOGY

LTE supports both frequency division duplex (FDD) and time division duplex (TDD) transmission modes. It uses orthogonal frequency division multiple access (OFDMA) which is a form of orthogonal frequency division multiplexing (OFDM) for multiuser communication. OFDM provides high data rate whilst coping with frequency selectivity of the channel by dividing the bandwidth into multiple orthogonal subcarriers. In OFDM, the binary data is coded and mapped to modulation symbols and then reshaped into parallel data. Pilot symbols are inserted for channel estimation and then an inverse fast Fourier transform (IFFT) of size  $N$  transforms the data into time domain. A replica of the last part of each OFDM symbol (known as cyclic prefix (CP)) is appended to the beginning of the symbol to prevent inter-symbol interference (ISI). At the receiver, the CP is removed from the signal distorted by a fading channel and additive white Gaussian noise (AWGN). The resultant signal undergoes a fast Fourier transform (FFT) operation to be transformed back into frequency domain. Finally, channel effects are eliminated by channel estimation and equalization and the equalized symbols are demodulated and decoded to obtain the binary data. Fig. 1 shows a typical block diagram of a baseband OFDM system.

In LTE, the spacing between adjacent subcarriers ( $\Delta f$ ) is 15 kHz (7.5 kHz in special cases) and each twelve consecutive subcarriers are grouped into a physical resource block (RB). In the time dimension, a radio frame consists of twenty time slots of length 0.5 ms each while a subframe has duration  $T_{LTE} = 1$  ms and consists of two consecutive slots, i.e., ten subframes form a radio frame of 10 ms duration [12]. Each time slot consists of six or seven OFDM symbols depending on whether an extended or normal cyclic prefix is used. Channel estimation is performed by inserting pilot symbols (known as cell specific RS (CRS) in LTE terminology) into the downlink (DL) signal to allow coherent demodulation at the user equipment (UE). This method, which is usually referred to as pilot-symbol aided channel estimation (PSACE), depends on estimating the channel at pilot locations and then performing interpolation in frequency and/or time domains to estimate the channel at the information-bearing parts of the signal. Several estimators can be used such as least square (LS), minimum mean square error (MMSE) estimator, etc. while the interpolation can be performed by linear interpolator, second order polynomial interpolator, spline cubic interpolator, etc. For comparisons between different types of estimators and interpolators in terms of their complexity and performance see [13] and [14] and the references therein.

Recalling the OFDM model of Fig. 1, the received signal after FFT operation is expressed as [13]:

$$Y(k) = X(k)H(k) + W(k) \quad , \quad k = 0, 1, \dots, N-1 \quad (1)$$

where  $Y(k)$ ,  $X(k)$  and  $H(k)$  are the received signal, the transmitted signal and the channel frequency response at subcarrier  $k$  respectively in the frequency domain.  $W(k)$  is the  $k^{\text{th}}$  subcarrier frequency domain noise component which is modelled as AWGN with zero mean and variance  $\sigma_n^2$ . In this paper, we consider the LS estimator that estimates the channel by the following formula [13].

$$\tilde{H}_p = \frac{Y_p}{X_p} = H_p + \frac{W_p}{X_p} \quad (2)$$

where the subscript  $p$  means the estimation is performed at the pilot locations only. For data subcarrier  $k$ , a linear interpolation method can be used to estimate the channel  $\tilde{H}(k)$  [14].

$$\tilde{H}(k) = \tilde{H}_p(m) + \frac{l}{L} \left( \tilde{H}_p(m+1) - \tilde{H}_p(m) \right) \quad (3)$$

where  $mL \leq k < (m+1)L$  and  $0 < l < L$  with  $L$  being the frequency spacing between two consecutive pilot subcarriers. Once the channel is estimated, a zero forcing (ZF) equalizer can be used to estimate the originally transmitted signal.

$$\tilde{X}(k) = \frac{Y(k)}{\tilde{H}(k)} \quad (4)$$

PSACE systems performance depends on the used estimator, interpolator, equalizer as well as the pilot pattern. The latter is constrained in the time and the frequency domains by coherence time  $T_c$  and coherence bandwidth  $B_c$  of the channel respectively. The coherence time is “a statistical measure of

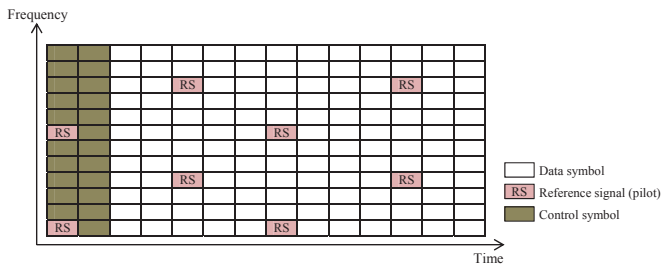


Fig. 2. LTE RB pair : one antenna port with CRS and control symbols [12].

the time duration over which the channel impulse response is essentially invariant” [15]. It is inversely proportional to the maximum Doppler shift  $f_d$  which itself depends on the UE speed  $v$  and the carrier frequency  $f$ .

$$T_c = \frac{1}{2f_d} \quad (5)$$

with

$$f_d = \frac{vf}{c} \quad (6)$$

where  $c$  is the speed of light. On the other hand, the coherence bandwidth defines the channel frequency selectivity level and it is inversely proportional to rms delay spread of the channel  $\sigma_\tau$ . If  $B_c$  is defined as the range of frequencies over which the frequency correlation function is above 0.9, then  $B_c$  is approximately [15]:

$$B_c = \frac{1}{50\sigma_\tau} \quad (7)$$

Based on these constraints, the maximum pilot spacing in the time and the frequency domains ( $N_t$  and  $N_f$  respectively) can be formulated as:

$$N_t \leq \frac{c}{2vf} \quad (8)$$

$$N_f \leq \frac{1}{50\sigma_\tau} \quad (9)$$

The pilot symbols (or CRS) have been distributed in the LTE resource grid based on high mobility assumptions and macro cell parameters: 500 km/hr speed and 991 ns rms delay spread [16]. Substituting these values into (5), (6) and (7) with  $f = 2$  GHz yields:  $f_d \approx 927$  Hz,  $T_c \approx 0.5$  ms and  $B_c \approx 20$  kHz. This implies that each time slot requires two CRS in the time domain while in the frequency domain there is one staggered CRS every three subcarriers [12]. In LTE Release-9, UE specific RS (UE-RS) is proposed for data demodulation purposes. It is transmitted in the RBs that contain user data and it replaces the CRS in the Lean Carrier [10]. Fig. 2 shows LTE RB pair (subframe with twelve subcarriers) for one antenna port with CRS and control symbols.

The control symbols are used in the DL for resource assignment and frame control related operations, and they occupy the first one, two, or three OFDM symbols of each subframe. For overhead calculations and comparisons with other frames, we consider the control and pilot symbols, the guard period (GP) and the CP as the relevant components that decrease the power and bandwidth efficiencies. Other signals for synchronization,

broadcast, etc. contribute to the overhead but they are not included for simplicity. LTE overhead depends on the number of used antennas as well as the frame configuration. In this paper, we consider one antenna port and TDD mode with special subframe configuration #0 (three DL pilot symbols, one uplink (UL) pilot symbol and ten symbols as a GP), see [12] for all possible LTE configurations. It can be noticed that the special subframe overhead is 100% while the overheads of the UL and the DL subframes depend on their allocations. To conduct a fair comparison, we calculate the average subframe overhead by considering the overhead of the radio frame, and we assume that the UL subframes have the same allocations as the DL subframes. Under such configuration, the average LTE subframe overhead can be formulated as:

$$overhead_{LTE} = \frac{X((N_{ctrl} + P)T_u + N_{sym}T_{cp}) + N_{sp}T_{LTE}}{10T_{LTE}} \quad (10)$$

where  $N_{sp}$  is the number of special subframes in a radio frame,  $X$  is the number of UL and DL subframes in a radio frame ( $X = 10 - N_{sp}$ ),  $N_{sym}$  is the total number of OFDM symbols in a subframe,  $N_{ctrl}$  is the number of control symbols in a subframe,  $T_{cp}$  is the CP duration,  $T_u = \frac{1}{\Delta f}$  is the useful OFDM symbol duration and  $P$  is the average number of data plane pilots per subframe. Notice that each subcarrier may or may not contain pilots according to the constraint of (9). The subframe overhead should account for both cases by dividing the total pilots in a RB pair by the number of subcarriers per RB ( $N_{sc}$ ). i.e.,

$$P = \frac{\bar{N}_p}{N_{sc}} \quad (11)$$

where  $\bar{N}_p$  is the number of pilot symbols in the data plane of a RB pair (i.e., excluding the pilots included in  $N_{ctrl}$ ).

### III. NEXT GENERATION FRAME IN SIGNALLING-DATA SEPARATION ARCHITECTURE

Reference [7] proposes a functionality separation scheme where a large signalling cell provides the coverage and its related low rate signalling information while dedicated data cells (within the signalling cell coverage) provide high rate data transmission. The signalling cell supports synchronization, broadcast, multicast, paging, handover and radio resource control (RRC) functions and therefore the signalling cell frame contains synchronization signals, pilot symbols, frame control, paging signal, broadcast and multicast data. On the other hand, the data cell provides high rate data transmission to active users only. As a result, only synchronization signals, pilot symbols, frame control and unicast data are required in the data cell frame. Fig. 3 shows a high level scenario for session establishment and data transmission under such separation scheme.

This paper focuses on the channel estimation performance of the data cell and therefore we ignore the signalling cell as well as the synchronization signal. The TDD subframe structure proposed in [11] is adopted and then adapted to the data cell. In this subframe,  $N_{ctrl}$  control symbols for transmit

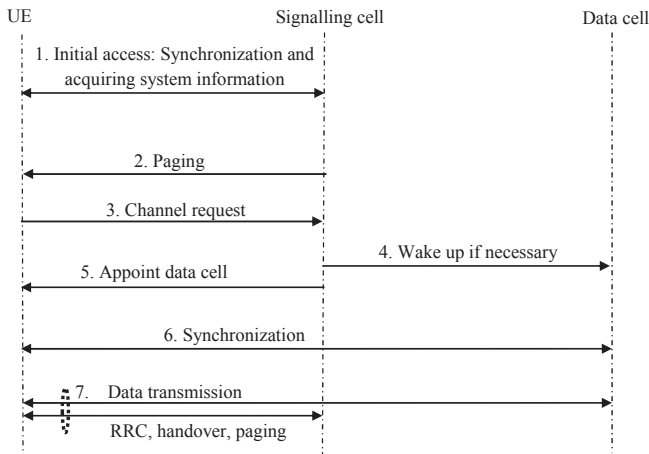


Fig. 3. High level scenario for call establishment and data transmission in signalling-data separation architecture

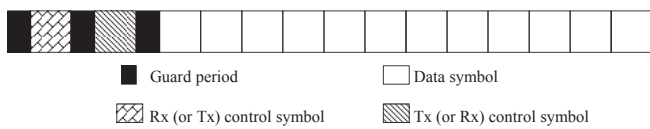


Fig. 4. TDD subframe for next generation cellular systems [11]

(Tx) and receive (Rx) are separated by a guard period  $T_{GP}$  and they are embedded to each subframe. The data part contains  $N_{data}$  symbols and it is used for Tx or Rx only and time separated by  $T_{GP}$  from the control plane. Considering OFDM as an access technique candidate for NG cellular systems [11], each symbol in the time/frequency grid consists of useful OFDM symbol with duration  $T_u$  and CP with duration  $T_{cp}$ . Fig. 4 shows the structure of this subframe (denoted by NG subframe in the rest of the paper) whose duration  $T_{NG}$  is formulated as [11]:

$$T_{NG} = (2N_{ctrl} + N_{data})(T_u + T_{cp}) + 3T_{GP} \quad (12)$$

$T_{GP}$  copes with the propagation delay  $T_{PD}$ , channel delay spread  $\sigma_\tau$ , filter response time to delay spread  $T_{FR}$  as well as the hardware switching time  $T_{H\_ST}$ . On the other hand, the CP eliminates the ISI and hence it should be larger than  $\sigma_\tau$  and  $T_{FR}$ . Following the argument of [17], in a small cell environment precise timing procedures may not be required if the two way propagation delay and other synchronization errors  $T_{sync}$  can be compensated by the CP. Thus the lower bounds for  $T_{GP}$  and  $T_{cp}$  can be formulated as [17]:

$$T_{GP} = \sigma_\tau + T_{PD} + T_{FR} + T_{H\_ST} \quad (13)$$

$$T_{cp} = \sigma_\tau + 2T_{PD} + T_{FR} + T_{sync} \quad (14)$$

For channel estimation, the time constraint of (8) can be used to set a lower bound for the number of pilots in a subframe in the time domain ( $N_{P,t}$ ).

$$N_{P,t} = \left\lceil \frac{T_{NG}}{T_c} \right\rceil = \left\lceil \frac{2vf((2N_{ctrl} + N_{data})(T_u + T_{cp}) + 3T_{GP})}{c} \right\rceil \quad (15)$$

TABLE I  
PARAMETERS OF THE LA AND MACRO CELLS

Parameter	LA cell	Macro cell
Cell radius (m)	50	250
$v$ (km/hr)	30	500
$\sigma_\tau$ (ns)	100	991
$\Delta f$ (kHz)	60	20

where  $\lceil x \rceil$  means the nearest integer that is not smaller than  $x$  (i.e., ceil operator). For a given RB bandwidth ( $BW_{RB} = \Delta f \cdot N_{sc}$ ), the frequency constraint of (9) can be used to set a lower bound for the number of pilots in a RB in the frequency domain ( $N_{P,f}$ ).

$$N_{P,f} = \left\lceil \frac{BW_{RB}}{B_c} \right\rceil = \lceil 50 \sigma_\tau \Delta f N_{sc} \rceil \quad (16)$$

Finally, the NG subframe overhead is calculated in a similar way as the LTE overhead by considering the duration of the non-data symbols w.r.t. the total subframe duration.

$$overhead_{NG} = \frac{(2N_{ctrl} + P)T_u + N_{sym}T_{cp} + 3T_{GP}}{T_{NG}} \quad (17)$$

where  $P$  has the same definition of (11).

#### IV. SUBFRAME ALLOCATIONS AND SIMULATION PARAMETERS

For overhead comparisons, we consider LTE TDD mode with 5 ms switch periodicity and UL/DL configuration #2 (i.e., six DL subframes, two special subframes and two UL subframes) [12]. Typical LTE parameters are considered: normal cyclic prefix  $T_{cp} = 4.7 \mu s$ ,  $N_{sym} = 14$ ,  $T_u = 66.7 \mu s$ ,  $N_{ctrl} = 2$  and  $\bar{N}_P = 6$  for CRS and 12 for UE-RS [12]. On the other hand, two cells are considered for the NG subframe. A small LA cell for low speed users (with a subframe denoted by NG LA) and a macro cell for high speed users (with a subframe denoted by NG Macro). Table I shows the parameters of each cell. In addition, the mutual parameters between the NG subframes of both cells are:  $T_{FR} = 50 \text{ ns}$ ,  $T_{H\_ST} = 60 \text{ ns}$  and  $T_{sync} = 500 \text{ ns}$  [17]. To conduct a fair comparison with the LTE, 14 symbols are considered for each subframe with  $N_{data} = 12$  and  $2 \cdot N_{ctrl} = 2$ .

Considering these parameters in conjunction with the formulas of Sections II and III, the LA cell has  $T_c = 9 \text{ ms}$  and its NG LA subframe has duration  $T_{NG} = 0.1 \text{ ms}$ , which results into  $N_{P,t} = 1$ . With  $\Delta f = 60 \text{ kHz}$  and  $B_c = 200 \text{ kHz}$ , every three subcarriers require one pilot symbol. As a result, all the pilot symbols can be accommodated in the control part (i.e.,  $\bar{N}_P = 0$ ) whilst ensuring there are enough resources for control signalling. On the other hand,  $T_c = 0.5 \text{ ms}$  and  $B_c = 20 \text{ kHz}$  in the macro cell while its NG Macro subframe has duration  $T_{NG} = 0.76 \text{ ms}$  with  $\Delta f = 20 \text{ kHz}$ . This implies that two pilot symbols are required in the time domain in each subcarrier (i.e.,  $N_{P,t} = 2$  and  $N_{P,f} = N_{sc}$ ). In contrast to the NG LA subframe, the pilot symbols can only be placed in the data part of the NG Macro subframe, otherwise the control part

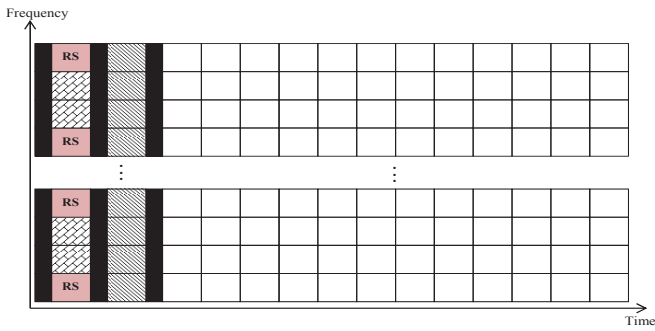


Fig. 5. NG LA subframe

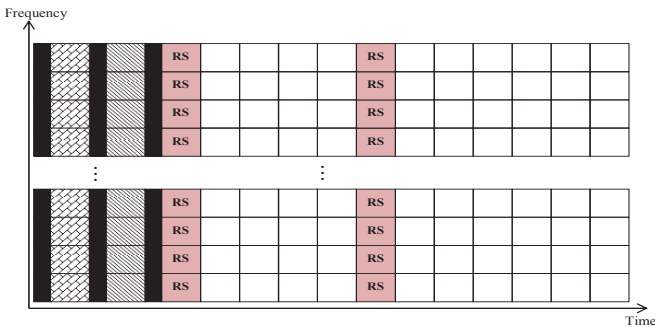


Fig. 6. NG Macro subframe

will be filled with pilot symbols. Notice that  $P$  simplifies to 0 and 2 in the NG LA and NG Macro subframes respectively. In other words, the NG subframes overhead is independent of  $N_{sc}$ . The allocations of the NG LA and the NG Macro subframes are shown in Figs. 5 and 6 respectively with the same legend of Fig. 4.

For performance comparisons, the OFDM model of Fig. 1 is considered along with the subframe structures of Figs. 2, 5 and 6. Other simulation parameters are provided in Table II.

## V. RESULTS

The simulations are performed using the same bandwidth of 20 MHz (including 10% as a guard band), which implies that different subframes with different subcarrier spacings would have different FFT sizes. To conduct a fair comparison, a FFT size of 2048 is considered whilst altering the used subcarriers for each subframe to ensure an occupied bandwidth of 18 MHz (i.e., total bandwidth of 20 MHz). The LTE channel models developed by the 3GPP are used in the simulation. These models are: Extended Pedestrian-A (EPA) which is used to model small cell environment ( $\sigma_\tau = 43$  ns), Extended Vehicular-A (EVA) and Extended Typical Urban (ETU) which are used to model urban environments with large cells ( $\sigma_\tau = 357$  ns and 991 ns respectively). The Doppler frequencies for these models with low, medium and high Doppler conditions are 5 Hz, 70 Hz and 900 Hz respectively. The following combinations are suggested in [18]: EPA–5 Hz, EVA–5 Hz, EVA–70 Hz and ETU–70 Hz. We consider EPA–5 Hz environment to compare the NG LA subframe with the LTE in a small cell scenario while EVA–70 Hz is considered in comparing the

TABLE II  
SIMULATION PARAMETERS

Parameter	LTE	NG LA	NG Macro
Modulation	QPSK		
Coding	$\frac{1}{2}$ rate Trellis code		
Estimator	Least square		
Interpolator	Linear (in frequency domain only)		
Equalizer	Zero forcing		
Channel model	Rayleigh channel (EPA and EVA)		
Doppler shift (Hz)	5 and 70		
Total bandwidth (MHz)	20		
Guard band (%)	10		
Occupied bandwidth (MHz)	18		
FFT size	2048		
Subcarrier spacing (kHz)	15	60	20
Used subcarriers	1200	300	900
Cyclic prefix ( $\mu$ s)	4.7	0.98	3.2
Guard period ( $\mu$ s)	NA	0.377	1.93

TABLE III  
EPA AND EVA POWER DELAY PROFILES

Tab No.	EPA		EVA	
	power (dB)	delay (ns)	power (dB)	delay (ns)
1	0	0	0	0
2	-1	30	-1.5	30
3	-2	70	-1.4	150
4	-3	80	-3.6	310
5	-8	110	-0.6	370
6	-17.2	190	-9.1	710
7	-20.8	410	-7	1090
8	NA	NA	-12	1730
9	NA	NA	-16.9	2510

LTE with the NG Macro subframe in a large cell / high speed scenario. Table III shows the power delay profiles of the EPA and EVA channel models.

Fig. 7 shows the bit error rate (BER) performance of the NG LA subframe and the LTE subframe in EPA–5 Hz scenario while Fig. 8 compares their overhead. As can be seen, in a small cell / low speed scenario the NG LA subframe provides roughly the same BER performance as the LTE subframe with a maximum degradation of 3%. From overhead perspective, the NG LA subframe reduces the overhead by 50% and 53% as compared with the LTE with CRS and LTE with UE-RS respectively. In other words, low speed users in small cells can achieve the same LTE performance with half of the overhead. This indicates that the power and bandwidth efficiencies can be increased significantly without noticeable performance degradation.

Fig. 9 compares the BER performance of the LTE subframe with the NG Macro subframe in the large cell / high speed scenario (i.e., EVA–70 Hz). As indicated by Figs. 8 and 9, the NG Macro subframe reduces the overhead by 10% and 16% as compared with the LTE with CRS and LTE with UE-RS

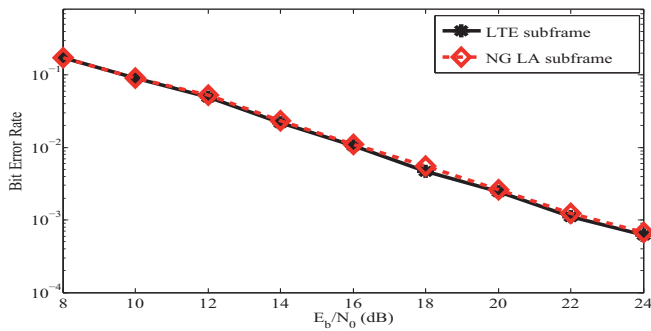


Fig. 7. Bit error rate of NG LA and LTE subframes in EPA-5Hz scenario

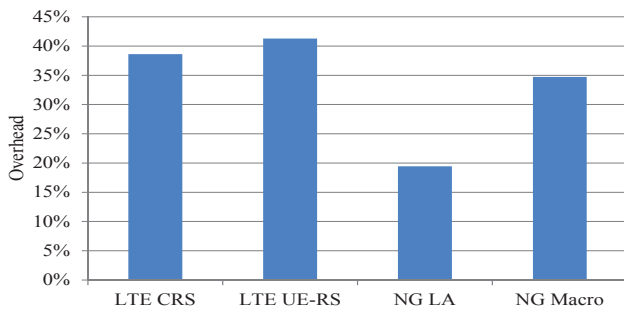


Fig. 8. Subframes overhead

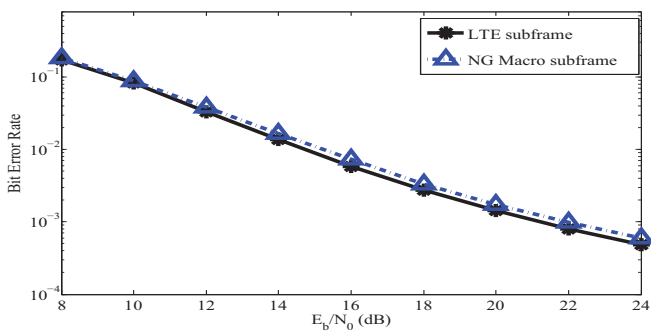


Fig. 9. Bit error rate of NG Macro and LTE subframes in EVA-70Hz scenario respectively at the expense of slight increase in the BER.

## VI. CONCLUSION

In this paper, we discussed the signalling-data separation architecture in conjunction with a PL subframe optimized for NG cellular systems. A review of the LTE PL frame structure is given along with the channel estimation method in LTE and OFDM systems. The overhead of both the LTE and the NG subframes are formulated whilst conforming to the time and the frequency constraints of the pilot pattern. Focusing on the channel estimation performance, simulation results depict that using a worst-case and unified frame structure optimized for macro coverage results into unnecessary overhead that can be eliminated without noticeable performance penalty. Precisely, up to 53% of the LTE overhead can be reduced without significant degradation in the BER performance. Such an architecture with a reduced overhead increases the spectral

efficiency and minimizes the energy consumption which helps in achieving the objectives of NG cellular systems.

## ACKNOWLEDGMENT

This work was made possible by NPRP grant No. 5-1047-2437 from the Qatar National Research Fund (a member of The Qatar Foundation). The statements made herein are solely the responsibility of the authors.

## REFERENCES

- [1] G. Fettweis and E. Zimmermann, "ICT energy consumption-trends and challenges," in *Proceedings of the 11th International Symposium on Wireless Personal Multimedia Communications*, vol. 2, no. 4, 2008, pp. 6–9.
- [2] EARTH project, "Deliverable d3.3: Final report on green network technologies," 2012. [Online]. Available: [https://bscw.ict-earth.eu/pub/bscw.cgi/d70472/EARTH\\_WP3\\_D3.3.pdf](https://bscw.ict-earth.eu/pub/bscw.cgi/d70472/EARTH_WP3_D3.3.pdf)
- [3] A. Capone, A. Fonseca dos Santos, I. Filippini, and B. Gloss, "Looking beyond green cellular networks," in *Proceedings of the 9th Annual Conference on Wireless On-demand Network Systems and Services*, 2012, pp. 127–130.
- [4] H. Ishii, Y. Kishiyama, and H. Takahashi, "A novel architecture for LTE-B: C-plane/U-plane split and Phantom Cell concept," in *IEEE Globecom Workshops*, Dec 2012, pp. 624–630.
- [5] J. Andrews, H. Claussen, M. Dohler, S. Rangan, and M. Reed, "Femtocells: Past, present, and future," *IEEE Journal on Selected Areas in Communications*, vol. 30, no. 3, pp. 497–508, April 2012.
- [6] Wunder, G. et al., "5GNOW: non-orthogonal, asynchronous waveforms for future mobile applications," *IEEE Communications Magazine*, vol. 52, no. 2, pp. 97–105, February 2014.
- [7] X. Xu, G. He, S. Zhang, Y. Chen, and S. Xu, "On functionality separation for green mobile networks: concept study over LTE," *IEEE Communications Magazine*, vol. 51, no. 5, pp. 82–90, 2013.
- [8] T. Zhao, P. Yang, H. Pan, R. Deng, S. Zhou, and Z. Niu, "Software defined radio implementation of signaling splitting in hyper-cellular network," in *Proceedings of the 2nd Workshop on Software Radio Implementation Forum*. New York, USA: ACM, 2013, pp. 81–84.
- [9] M. Olsson, C. Cavdar, P. Frenger, S. Tombaz, D. Sabella, and R. Jantti, "5Green: Towards green 5G mobile networks," in *Proceedings of the IEEE 9th International Conference on Wireless and Mobile Computing, Networking and Communications*, 2013, pp. 212–216.
- [10] C. Hoymann, D. Larsson, H. Koorapaty, and J.-F. Cheng, "A lean carrier for LTE," *IEEE Communications Magazine*, vol. 51, no. 2, pp. 74–80, 2013.
- [11] E. Lahtekangas, K. Pajukoski, E. Tirola, G. Berardinelli, I. Harjula, and J. Vihriala, "On the TDD subframe structure for beyond 4G radio access network," in *Proceedings of the Future Network and Mobile Summit*, 2013, pp. 1–10.
- [12] 3GPP, "Ts 36.211: Evolved universal terrestrial radio access (E-UTRA): Physical channels and modulation," Technical specification, ETSI, 2013. [Online]. Available: <http://www.3gpp.org/DynaReport/36211.htm>
- [13] J. van de Beek, O. Edfors, M. Sandell, S. Wilson, and P. Ola Borjesson, "On channel estimation in OFDM systems," in *Proceedings of the IEEE 45th Vehicular Technology Conference*, 1995, pp. 815–819.
- [14] S. Coleri, M. Ergen, A. Puri, and A. Bahai, "A study of channel estimation in OFDM systems," in *Proceedings of the IEEE 56th Vehicular Technology Conference*, 2002, pp. 894–898.
- [15] T. S. Rappaport, *Wireless communications: principles and practice*. Prentice Hall, New Jersey, 1996.
- [16] F. Khan, *LTE for 4G mobile broadband: air interface technologies and performance*. Cambridge University Press, 2009.
- [17] E. Lahtekangas, K. Pajukoski, G. Berardinelli, F. Tavares, E. Tirola, I. Harjula, P. Mogensen, and B. Raaf, "On the selection of guard period and cyclic prefix for beyond 4G TDD radio access network," in *Proceedings of the 19th European Wireless Conference*, 2013, pp. 1–5.
- [18] Ericsson, Rohde and Schwarz, Nokia, and Motorola, "R4-070572: Proposal for LTE channel models," 3GPP TSG RAN WG4, meeting 43, 3GPP, Kobe, Japan, 2007. [Online]. Available: <http://www.3gpp.org/DynaReport/TDocExMtg--R4-43--26006.htm>